

Foundation Flexibility Effects on the Seismic Response of Concrete Gravity Dams

by

José A. Inaudi¹, Enrique E. Matheu², Rick L. Poeppelman³, and Ariel Matusевич¹

ABSTRACT

This paper presents advances in an ongoing research project on simplified linear methods for preliminary seismic analysis of dams. In particular, several aspects of the influence of foundation flexibility on the seismic response of concrete gravity dams are addressed. Finite elements models, continuum-parameter models, and three degree-of-freedom models are used to evaluate the dynamic behavior of concrete gravity monoliths on flexible foundations. Hydrodynamic phenomena are modeled using frequency-domain representations of the semi-infinite reservoir accounting for fluid compressibility and reservoir-bottom energy absorption. The effects of foundation flexibility on seismic response are investigated, analyzing the fundamental mode shape and effective mass of the dam-foundation model for horizontal ground motion. The effect of the rocking and translation components of the fundamental mode shape on hydrodynamic pressure and base shear is characterized comparing displacement and base shear frequency response functions for different foundation flexibilities.

A simplified method to estimate the period elongation, added damping due to hydrodynamic interaction, and distribution of inertial forces is recommended using a standard mode shape that includes the effect of rocking and base displacement due to foundation flexibility. Accuracy of the proposed single mode analysis is evaluated comparing frequency response functions of dam-crest relative displacement and seismic base shear.

KEYWORDS: Seismic Response; Concrete Gravity Dams; Foundation Flexibility; Dam-Foundation Interaction.

1. INTRODUCTION

The influence of foundation flexibility on the dynamic response of massive concrete structures may be very significant. For example, in the case of concrete gravity dams for which the ratio between the modulus of elasticity of the foundation, E_f , and that of the dam, E_s , is smaller than one, important rocking components can be expected in the vibration response. This may have a considerable effect on the dynamic performance of gravity monoliths subjected to seismic ground motion.

Preliminary design and evaluation of concrete gravity sections is usually performed using the simplified response spectrum method proposed by Fenves and Chopra (1986). A standard fundamental mode of vibration, representative of typical sections, is used in this method. This mode shape does not take into account the foundation flexibility since it is representative of a standard concrete gravity section on rigid foundation. As an alternative, the first mode of vibration of the concrete section could be estimated using a finite element model with massless foundation. In the case of relatively flexible foundations, an important rocking component can be observed in the computed fundamental mode shape. The rocking response component caused by base rotation may induce significant differences in the effective mass and inertial-force distribution. Therefore, the use of the computed mode shape in the simplified

¹ SIRVE Vibration Reduction Systems, Córdoba, X5000KLJ (Argentina)

² U.S. Army Engineer Research and Development Center, Vicksburg, MS 39180 (USA)

³ U.S. Army Corps of Engineers, Sacramento District, Sacramento, CA 95814 (USA)

analysis, instead of the standard mode shape, may lead to considerable variations in the estimation of seismic demands such as base shear and overturning moment. This observation motivated the research reported in this paper.

2. FOUNDATION FLEXIBILITY EFFECTS ON MODE SHAPES

2.1 Finite Element Model

A two-dimensional (2D) finite-element (FE) model is used to investigate the effects of foundation flexibility on the fundamental mode of vibration of a typical non-overflow gravity section with empty reservoir. The dam height is 100 meters, the downstream slope is 0.78:1, and the upstream face is assumed vertical for simplicity. The crest of the dam is 9.36 m wide, and a rectangular section is assumed for the top 12 m of the monolith. Standard material properties are assumed, with unit weight of concrete = 2.53 ton/m³, and $E_s = 3,515,400$ ton/m². Radiation damping in the foundation is not considered in the study.

Figure 1 shows the FE mesh of triangular quadratic elements in plane strain and the computed first-mode lateral displacement along the upstream face for different ratios $E_f / E_s = 0.3, 0.5, 1, 2, 5, \infty$ (solid lines). The circles correspond to the standard mode shape recommended for non-overflow sections in Chopra's simplified procedure (Fenves and Chopra, 1986). Foundation flexibility causes significant lateral displacement and rotation at the base of the dam in the fundamental mode that deviates significantly from the standard mode (which corresponds to fixed-base conditions), especially for $E_f / E_s < 1$.

The change in natural frequency due to foundation flexibility can be estimated using the coefficient R_f recommended by Chopra in the simplified method. However, the estimation of base shear, hydrodynamic pressure, and inertial force distribution highly depends on the effective modal masses and mode shape, which

in the simplified procedure are considered as that of a fixed-base dam.

For the example considered, the normalized effective masses for lateral motion corresponding to the first mode of vibration are computed as $m_{e1x} = 0.85, 0.73, 0.56, 0.46, 0.40, 0.36$, for ratios $E_f / E_s = 0.3, 0.5, 1, 2, 5, \infty$, respectively. Using the standard mode shape, the normalized effective modal mass for this section is 0.447 (independent of foundation flexibility).

2.2 Continuum Parameter Model

As an alternative approach for modal analysis, a model of the dam section is developed using the theory of beams with plane sections, shear deformation, and coupled axial and flexural vibrations due to cross-section asymmetry. Warping is neglected, and the motion of plane sections is described by a vertical displacement field, $u_y(y, t)$, a lateral displacement field, $u_x(y, t)$, and a rotation field, $\psi_z(y, t)$ (**Figure 2**).

The lateral stiffness, vertical stiffness, and rotational stiffness of the foundation are assumed as those of a square foundation (with dimensions $2b \times 2b$) on a semi-infinite elastic medium at low frequencies (Richart et al., 1970)

$$\begin{aligned} k_h &= 2E_f b \\ k_v &= 4.3E_f b / 2(1 + \nu_f)(1 - \nu_f) \\ k_\theta &= 2E_f b^3 / (1 + \nu_f)(1 - \nu_f) \end{aligned} \quad (1)$$

where ν_f = Poisson ratio of the foundation.

Using Hamilton's principle, a set of coupled partial differential equations and corresponding boundary conditions are obtained for the displacement fields. The application of the method of separation of variables leads to the differential equations for the mode shapes and natural frequencies. Details, not included here for brevity, can be found in a paper by Inaudi and Matusевич (2005).

Table 1 compares the natural periods and normalized effective masses in horizontal and vertical directions for the first mode of vibration estimated with this procedure and the FE model as functions of the ratio E_f/E_s . The table shows that the difference between the natural period estimates provided by the models becomes larger as the foundation flexibility increases (i.e., E_f/E_s decreases). The table also shows that the trend of increasing effective modal mass with foundation flexibility is confirmed by both models.

It was determined that cross-section warping did not have a significant influence on the difference observed in the fundamental period estimates. This was confirmed by imposing plane-section constraints on the dam-foundation interface in the FE model and computing the corresponding vibration periods. For example, the first natural period for $E_f/E_s = 0.3$ changed only from 0.419 s to 0.409 s.

To investigate the influence of effective width of the foundation on its stiffness, let us consider stiffness estimates for rectangular foundations (with dimensions $B \times L$) as given by Wolf and Meek (1994) and a Department of Defense Manual (1983), maintaining a constant monolith base B and varying the equivalent width L . **Figure 3** shows the corresponding lateral and rocking stiffness normalized by the foundation width. The results show larger flexibility per unit width as the width L of the rigid foundation increases. Concrete gravity monoliths interact through the foundation rock and contraction joints. Assuming that adjacent monoliths of similar height show synchronous motion, foundation stiffness estimates for a single monolith on an isolated foundation will show some overestimation because the width of the single monolith would be used in the computation of its corresponding foundation stiffness. The equivalent stiffness per unit width of a single monolith is clearly larger than the stiffness per unit width of two or more monoliths (much larger L/B) with synchronous motion (as shown in **Figure 3**). In the limit, the

foundation stiffness for $L/B \rightarrow \infty$ should converge to the stiffness estimated by a 2D FE model with a plane-strain foundation region. The values shown between parentheses in **Table 1** correspond to models with foundation stiffness adjusted to the values obtained from a 2D FE analysis of a rigid foundation, neglecting coupling of the condensed stiffness matrix. These values are closer to the 2D FE estimates in fundamental period of vibration and effective lateral mass.

The main reason for the difference in the computed periods shown in **Table 1** is that the representation of foundation flexibility effects in the 2D FE model and the approximate model based on analytical expressions for a square isolated foundation differ significantly. These foundation modeling approaches are simplified strategies to represent the actual 3D system constituted by the concrete gravity monoliths and the foundation rock. A single monolith or a set of adjacent monoliths do not behave as supported by isolated square foundations, or by a single rigid rectangular foundation of infinite out-of-plane width. Therefore, special attention should be paid when developing approximate models to represent the foundation region beneath single monoliths, particularly for those cases with relatively low values of E_f/E_s .

2.3 Simplified Foundation Model

Another simplified approach to estimate mode shapes and natural frequencies of a concrete gravity monolith, including foundation flexibility effects, is to use standard FE discretization techniques on the dam and represent the foundation elasticity by equivalent lumped elements at the center of gravity of the dam-foundation interface section. This model requires the incorporation of nodal displacement constraints enforcing rigid-body conditions along the base of the dam.

For low-frequency mode estimation, the parameters defined in Eq. (1) or other frequency-dependent dynamic stiffness expressions suggested in the literature can be

used. Because the rigid-body constraint along the dam-foundation interface does not have a significant effect on the lower natural frequencies, this type of model provides good estimates of low-frequency mode shapes and natural frequencies, provided that the lumped stiffness parameters are assumed adequately.

2.4 Simplified Dam-Foundation Model

The normalized effective mass in vertical motion of the fundamental mode of vibration of a typical dam on flexible foundation is relatively small, as shown in **Table 1**. In addition, vertical displacements due to rocking motion are not very significant. Therefore, a simplified 3-degree-of-freedom (3DOF) model that neglects vertical motion and captures the lateral and rocking components due to foundation flexibility can give satisfactory accuracy in the estimation of the fundamental mode of vibration. The model defines a horizontal displacement field as

$$u_x(x, y, t) = q_x(t) + \theta(t)y + q_s(t)\psi_{1s}(y) \quad (2)$$

where $q_x(t)$ = rigid body lateral displacement of the dam induced by the foundation, $\theta(t)$ = the rigid body rotation induced by the foundation, $\psi_{1s}(y)$ = Chopra's standard mode shape used in the simplified method, and $q_s(t)$ = the coordinate that represents dam deformation. For these coordinates, the stiffness matrix can be expressed as

$$\mathbf{K} = \begin{bmatrix} k_h & 0 & 0 \\ 0 & k_\theta & 0 \\ 0 & 0 & k_s \end{bmatrix} \quad (3)$$

where

$$k_s = (2\pi/T_{1s})^2 \int_0^{H_s} 2ba(y)\rho_s\psi_{1s}^2(y)dy \quad (4)$$

ρ_s = mass density of dam concrete, and T_{1s} = standard fundamental frequency of the dam on rigid foundation (Fenves and Chopra,

1986); $a(y)$ = width of the cross section of the dam; $B = 2b$ is the monolith base; and $L = 2b$ is the monolith thickness or width, assumed equal to B to use the stiffness of a square foundation defined in Eq. 1 (as discussed previously, the stiffness of a different equivalent rectangular foundation could be alternatively used).

Using the mass distribution of the dam and considering only horizontal motion of the dam (assumed independent of horizontal coordinate x), we obtain the corresponding mass matrix from the differentiation of the approximation of the kinetic energy

$$\mathbf{M} = 2b\rho_s \begin{bmatrix} \int_0^{H_s} a(y)dy & \int_0^{H_s} a(y)ydy & \int_0^{H_s} a(y)\rho_s\psi_{1s}(y)dy \\ \int_0^{H_s} a(y)ydy & \int_0^{H_s} a(y)y^2dy & \int_0^{H_s} a(y)y\psi_{1s}(y)dy \\ \int_0^{H_s} a(y)\rho_s\psi_{1s}(y)dy & \int_0^{H_s} a(y)y\psi_{1s}(y)dy & \int_0^{H_s} a(y)\psi_{1s}^2(y)dy \end{bmatrix} \quad (5)$$

Solving the standard eigenvalue problem, we obtain an estimate of the first natural period and mode shape of the dam taking into account foundation flexibility. The results obtained by this method are shown in **Table 1** and compared with the corresponding values obtained by the continuum model. As shown, an excellent fit is obtained with the continuum model described in the previous section.

Defining the first mode estimation as

$$\phi_1(y) = \beta_1 + \beta_2 y/H_s + \beta_3\psi_{1s}(y), \quad (6)$$

normalizing this first mode shape such that $\phi_1(H_s) = 1$, and considering that $\psi_{1s}(H_s) = 1$, then the estimated mode shape can be entirely defined by the coefficients β_1 and β_2 , with $\beta_3 = 1 - \beta_1 - \beta_2$.

Figure 4 shows the foundation flexibility effects on the lateral displacement component, β_1 , the rocking component, β_2 , and the deformation component β_3 corresponding to the first mode of vibration. The figure shows the first mode estimates obtained with both the continuum

model and the 3DOF model. If a finite-element model of the dam-foundation system is not available, then the mode shape computed with the 3DOF model is recommended for estimating inertial load distribution in simplified seismic analysis of dams and hydrodynamic loads, as we explain in the following section.

3. DAM-RESERVOIR INTERACTION

3.1 Hydrodynamic Pressure

The dynamics of a single monolith of a gravity dam can be efficiently modeled in planar motion. The horizontal acceleration of the boundary of the fluid domain in contact with the vertical upstream face of the dam (coordinate $x=0$) causes interaction between the dam and the reservoir. Let us define

$$\ddot{u}_x(y,t) = \ddot{u}_{gx}(t) + r_x(0,y,t) \quad (7)$$

where $\ddot{u}_x(y,t)$ = horizontal absolute motion of the upstream dam face, $\ddot{u}_{gx}(t)$ = free-field ground motion in the horizontal direction, and $r_x(0,y,t)$ = relative motion of the upstream dam face with respect to the free-field motion. This relative motion of the dam face can be modeled as a linear combination of N_q generalized coordinates $q_i(t)$ and Ritz fields (or finite-element shapes), $\psi_i(x,y)$, in a reduced-order finite-dimensional model of the dam as follows:

$$r_x(0,y,t) = \sum_{i=1}^{N_q} q_i(t)\psi_i(0,y) \quad (8)$$

In this study, the mode shapes of the dam-foundation model are used for order reduction because these coordinates show minor coupling, allow the estimation of the effects of reservoir interaction in a direct manner, and are suitable for spectral modal analysis.

Assuming a uniform vertical acceleration $\ddot{u}_{gy}(t)$ along the bottom of the reservoir, we can obtain the following frequency-domain

expression for the hydrodynamic pressure distribution on the dam face as a linear combination of the boundary motions of the reservoir:

$$P(y,\varpi) = H_{p\ddot{u}_{gx}}(y,\varpi)\ddot{U}_{gx}(\varpi) + \dots \\ H_{p\ddot{u}_{gy}}(y,\varpi)\ddot{U}_{gy}(\varpi) + \sum_{i=1}^{N_q} H_{p\ddot{q}_i}(y,\varpi)\ddot{Q}_i(\varpi) \quad (9)$$

where ϖ = frequency variable, $H_{p\ddot{u}_{gx}}(y,\varpi)$ = frequency response function (FRF) from horizontal ground acceleration (rigid dam face) to hydrodynamic pressure, $H_{p\ddot{u}_{gy}}(y,\varpi)$ = FRF from vertical ground acceleration (rigid reservoir bottom) to hydrodynamic pressure, and $H_{p\ddot{q}_i}(y,\varpi)$ = FRF from acceleration of modal coordinate $q_i(t)$ to hydrodynamic pressure $p(y,t)$ on the dam face. These frequency response functions depend on the generalized shapes used in the analysis.

Using virtual work, the load vector on the generalized modal coordinate $q_i(t)$ due to the hydrodynamic pressure can be expressed as

$$P_{q_i}(\varpi) = \int_0^{H_w} P(y,\varpi)\psi_i(y)dy \quad (10)$$

where H_w is the height of water in contact with the dam face. In vector notation then

$$\mathbf{P}_q(\varpi) = \mathbf{H}_{p\ddot{u}_{gx}}(\varpi)\ddot{U}_{gx}(\varpi) + \dots \\ + \mathbf{H}_{p\ddot{u}_{gy}}(\varpi)\ddot{U}_{gy}(\varpi) + \mathbf{H}_{p\ddot{q}_i}(\varpi)\ddot{\mathbf{Q}}(\varpi) \quad (11)$$

$\mathbf{H}_{p\ddot{u}_{gx}}(\varpi)$ and $\mathbf{H}_{p\ddot{u}_{gy}}(\varpi)$ are column vectors of N_q components, and $\mathbf{H}_{p\ddot{q}_i}(\varpi)$ is a square $N_q \times N_q$ matrix obtained by integration of Eq. (10) after replacing Eq. (9) into Eq. (10).

The frequency domain formulation of rectangular semi-infinite fluid domains (Eq. 9 and Eq. 10) has been investigated by several

authors. Details of the formulation can be found in the work by Fenves and Chopra (1984) where the effects of energy absorption in the bottom of the reservoir are considered and a comprehensive analysis of the reservoir-dam-foundation interaction is presented. The main parameters required for this formulation are H_w = height of water reservoir, ρ_w = density of water, C_w = speed of sound in water, and α = wave reflection coefficient for reservoir bottom absorption. To carry out the computations presented in this paper, a computer program was developed to evaluate the pressure frequency response functions, implementing this formulation.

Let us consider the hydrodynamic loads on the first mode of vibration of the dam-foundation system due to accelerations in the first modal coordinate. Variations in the fundamental mode shape of the dam monolith significantly affect this fluid-structure interaction problem, as shown in **Figure 5**, where the normalized real and imaginary components of the hydrodynamic load on the first modal coordinate due to acceleration of this modal coordinate are shown for two values of frequency and for different foundation flexibility values.

To better quantify the effect of foundation flexibility on hydrodynamic pressures, the added hydrodynamic mass on the first modal coordinate $-\text{real}(\mathbf{H}_{p,q\ddot{q}}[1,1])$ and the energy dissipation component $\text{imag}(\mathbf{H}_{p,q\ddot{q}}[1,1])$ are computed as functions of frequency and normalized with respect to the first modal mass m_1 to show the proportion of equivalent added hydrodynamic mass on the first modal coordinate due to dam-reservoir interaction and the energy dissipation of the first modal coordinate due to reservoir interaction (**Figure 6**). The normalized frequency is ϖ / ω_{r1} , where ω_{r1} = first natural frequency of the reservoir. Although the hydrodynamic pressure increases with the change in mode shape due to the increase in foundation flexibility (**Figure 4**), the relative increase of hydrodynamic mass with respect to modal mass decreases, because the

modal mass increases more rapidly with the increase of foundation flexibility.

Figure 7 shows the absolute value and the real part of $\mathbf{H}_{p,q\ddot{q}}[1]$ normalized by the ground-motion influence coefficient $L_{x1} = -\phi_1^T \mathbf{M} \mathbf{1}_x$ to assess the relative importance of the hydrodynamic pressure loading terms with respect to the direct seismic inertial load on the fundamental modal coordinate. As the figure shows, for values of ϖ / ω_{r1} close to 1, the hydrodynamic load on the first mode takes values close to the inertial effect of the ground motion on the dam with empty reservoir.

3.2 Coupled Dam-Reservoir System

The dynamic behavior of the dam-foundation-reservoir model can be expressed as

$$\mathbf{M}_q \ddot{\mathbf{Q}}(\varpi) + \mathbf{C}_q \dot{\mathbf{Q}}(\varpi) + \mathbf{K}_q \mathbf{Q}(\varpi) = \dots \quad (12)$$

$$\mathbf{P}_q(\varpi) - \Phi^T \mathbf{M} \mathbf{1}_x \ddot{U}_{gx}(\varpi) - \Phi^T \mathbf{M} \mathbf{1}_y \ddot{U}_{gy}(\varpi)$$

where \mathbf{M}_q , \mathbf{C}_q , and \mathbf{K}_q are the mass, damping and stiffness matrices of the dam-foundation model in modal coordinates; vectors $\mathbf{1}_x$ and $\mathbf{1}_y$ contain ones in the corresponding degrees of freedom of the dam (in direction x and y, respectively); the mass matrix \mathbf{M} contains only the mass contribution of the dam (massless foundation model).

Replacing Eq. (11) into Eq. (12), the following frequency-domain representation of the dynamics of the coupled system is obtained:

$$\left[-\varpi^2 (\mathbf{M}_q - \mathbf{H}_{p,q\ddot{q}}(\varpi)) + j\varpi \mathbf{C}_q + \mathbf{K}_q \right] \mathbf{Q}(\varpi) = \dots \quad (13)$$

$$\mathbf{H}_{p,q\ddot{q}}(\varpi) \ddot{U}_{gx}(\varpi) + \mathbf{H}_{p,q\ddot{q}}(\varpi) \ddot{U}_{gy}(\varpi) +$$

$$-\Phi^T \mathbf{M} \mathbf{1}_x \ddot{U}_{gx}(\varpi) - \Phi^T \mathbf{M} \mathbf{1}_y \ddot{U}_{gy}(\varpi)$$

Because the dam-foundation mode shapes are used in the formulation, matrices \mathbf{M}_q and \mathbf{K}_q are diagonal. If classical modal damping is defined for each mode, \mathbf{C}_q is also diagonal. In this work, 5% modal damping ratios are assumed for the

dam-foundation model, and foundation radiation damping is not considered.

Figure 8 shows a block diagram representation of the dynamics of the coupled dam-reservoir system (closed-loop system). By examining the frequency-domain representation in Eq. (13), a feedback component, given by $\mathbf{H}_{p,q\ddot{q}}(\varpi)$, can be identified in the dynamics of the coupled system which modifies the natural frequencies and damping ratios of the dam-foundation model.

Natural frequencies of the dam-foundation system are typically well separated (Inaudi and Matusевич, 2005), and modal coupling due to hydrodynamic pressure does not play a major role in seismic response and can be neglected without significant loss of accuracy. Therefore, neglecting modal interaction through the fluid (off-diagonal terms of the matrix $\mathbf{H}_{p,q\ddot{q}}(\varpi)$), the fundamental closed-loop system resonance frequency, $\hat{\omega}_1$, can be estimated by finding the frequency that makes the dynamic stiffness of the first modal coordinate equal to zero:

$$-\hat{\omega}_1^2(m_1 - \text{real}(\mathbf{H}_{p,q\ddot{q}}[1,1](\hat{\omega}_1))) + k_1 = \mathbf{0} \quad (14)$$

where k_1 and m_1 represent the first-mode stiffness and modal mass, respectively, of the dam-foundation model.

The contribution of the reservoir to the damping ratio of the approximate first modal equation can be estimated by equating the imaginary part of the modal dynamic stiffness to that corresponding to a viscous single-degree-of-freedom (SDOF) oscillator at $\varpi = \hat{\omega}_1$, to obtain

$$\begin{aligned} \hat{\xi}_{r,1} &= \frac{\hat{\omega}_1 \text{imag}(\mathbf{H}_{p,q\ddot{q}}[1,1](\hat{\omega}_1))}{2\hat{m}_1\hat{\omega}_1} \\ &= \frac{\text{imag}(\mathbf{H}_{p,q\ddot{q}}[1,1](\hat{\omega}_1))}{2(m_1 - \text{real}(\mathbf{H}_{p,q\ddot{q}}[1,1](\hat{\omega}_1)))} \end{aligned} \quad (15)$$

Let us define the coefficient R_r as the ratio of period of the coupled dam-reservoir system to

the period of the dam-foundation model. **Figure 9a** shows the variation of this coefficient as a function of E_f/E_s for a set of values of α , for the dam model previously used as an example. The figure shows that the coefficient R_r clearly depends on foundation flexibility. This is due to the mode shape dependence on the ratio E_f/E_s . The figure also shows that R_r becomes almost independent from the wave reflection coefficient α for $E_f/E_s < 0.5$.

In Chopra's simplified method, the period elongation of the dam-foundation-reservoir model is estimated by the product of two factors: R_f and R_r . The factor R_f depends on the ratio E_f/E_s and is independent of reservoir interaction effects, whereas R_r is independent of the flexibility of the foundation since it is based on the mode shape corresponding to rigid foundation conditions.

Figure 9b shows estimates of the damping ratio contribution associated with hydrodynamic effects (defined as $\hat{\xi}_{r,1}$ in this paper and ξ_r in Chopra's simplified method) for different values of α . Again, we notice that dam-reservoir interaction damping depends on the ratio E_f/E_s . This term is considered independent of foundation flexibility effects in Chopra's simplified procedure. As the figure shows, the change in this parameter due to foundation flexibility is not as significant as the change in R_r .

3.3 Equivalent SDOF Model

To compute the equivalent natural frequency of the first closed-loop mode shape, the first mode of vibration can be approximated by Eq. (6). The coefficients, β_1 , β_2 , and β_3 are computed by standard modal analysis of the dam-foundation model or solving the eigenvalue problem for the 3DOF model described in section 2.3.

The computation of $\mathbf{H}_{p,q\ddot{q}}[1,1]$ requires the evaluation of the integrals of the frequency-

response functions of the hydrodynamic pressure for the response components that define the fundamental mode, and this can be expressed as the following quadratic form

$$\mathbf{H}_{p,q\ddot{q}}[1,1](\varpi) = \begin{bmatrix} \beta_1 \\ \beta_2 \\ \beta_3 \end{bmatrix}^T [T_{HD}(\varpi)] \begin{bmatrix} \beta_1 \\ \beta_2 \\ \beta_3 \end{bmatrix} \quad (16)$$

where $T_{HD}(\varpi)$ is a symmetric 3x3 matrix whose terms are obtained by integrating along the height of the dam the frequency response functions between the generalized coordinates and the hydrodynamic pressure.

Because $T_{HD}(\varpi)$ is symmetric, only six different terms are required to define the full matrix. These terms are shown in **Figure 10** for $\alpha = 0.9$ and $H_w/H_s = 1$, as functions of normalized frequency and normalized by the reservoir height square and water density. Assuming these functions are available in tables or graphs similar to **Figure 10** for all ranges of parameters of interest, a general procedure can be proposed as follows:

- I. Compute the first mode of vibration and natural frequency ω_1 of the dam-foundation model to obtain the parameters $\beta_1, \beta_2, \beta_3, m_1$, and k_1 .
- II. Initialize $\hat{\omega}_1 = \omega_1$
- III. Compute normalized frequency estimate $R_w = \hat{\omega}_1 / \omega_{r1}$
- IV. From tables or graphs evaluate $T_{HD}(R_w)$ and compute $\mathbf{H}_{p,q\ddot{q}}[1,1]$ with the quadratic form in Eq. (16).
- V. Compute $\hat{\omega}_1$ using Eq. (14).
- VI. Return to III until convergence is achieved

Once the closed-loop natural frequency has been computed, $\hat{\xi}_{r1}$ can be computed applying Eq. (15). For the standard mode shape defined by β_1, β_2 , and β_3 , we can express

$$\begin{aligned} \text{imag}(\mathbf{H}_{p,q\ddot{q}}[1,1](\varpi)) &= \\ &= \begin{bmatrix} \beta_1 \\ \beta_2 \\ \beta_3 \end{bmatrix}^T \text{imag}[T_{HD}(\varpi)] \begin{bmatrix} \beta_1 \\ \beta_2 \\ \beta_3 \end{bmatrix} \quad (17) \end{aligned}$$

3.4 Hydrodynamic Loading Terms

In the frequency-domain representation defined in Eq. (13), four loading terms can be identified. Two of them are directly due to ground motion inertial effects, and they are standard in any seismic analysis problem. The other two loading terms, which are given by $\mathbf{H}_{p,q\ddot{u}_{gx}}(\varpi)\ddot{U}_{gx}(\varpi)$ and $\mathbf{H}_{p,q\ddot{u}_{gy}}(\varpi)\ddot{U}_{gy}(\varpi)$, constitute feed-forward components and they represent reservoir-filtered ground motion terms. They represent the pressure acting on the generalized coordinates due to the hydrodynamic pressure field produced by a rigid dam moving laterally and a rigid reservoir bottom moving vertically, respectively. The spectra corresponding to these reservoir-filtered ground motion signals will show peaks at the natural frequencies of the reservoir. Therefore, the frequency response functions from ground acceleration to a particular output of the system will show these peaks, which are not related to modes of vibration of the closed-loop system (fluid-structure interaction model) but to the feed-forward loop defined by the reservoir. These peaks are especially noticeable in the case of full-reservoir rigid dams (high E_s values or special monolith geometries that show a first natural frequency of the reservoir lower than the first frequency of the dam), and wave reflection coefficient α close to 1.

As these filters amplify the input signal at the natural frequencies of the reservoir, their effect on the dam response may be significant if the natural frequency of the reservoir coincides with the closed-loop frequency of the dam-foundation-reservoir system. This is not an unusual situation when H_w is close to H_s . The first natural period of a standard non-overflow dam monolith on rigid foundation is approximately (Fenves and Chopra, 1986)

$$T_1 = 1.4H_s / \sqrt{E_s} \quad (18)$$

for H_s in feet and E_s in psi. The fundamental natural period of the reservoir with $\alpha=1$ is

$$T_{r1} = 4H_w / C_w \quad (19)$$

Considering the speed of sound in water $C_w = 4,720$ ft/s (1,438.7 m/s), and from the last two equations, it can be shown that a value of $E_s = 2,729,104$ psi (1,918,750 ton/m²) yields identical values of natural periods for $H_s = H_w$. In addition, the closed-loop system fundamental period of the dam-reservoir system will be higher than T_1 due to reservoir added mass. This means that it could be possible to have a first natural period for the dam-reservoir system equal to the reservoir natural period for some value of E_s larger than 2,729,104 psi.

In the case of flexible foundation rock, the elongation of the natural period due to foundation flexibility and reservoir interaction will usually separate the closed-loop natural period from the reservoir natural period. Another consequence of this is related to the amount of added damping by the reservoir because the imaginary part of the hydrodynamic pressure FRF shows larger imaginary parts (dissipation) for frequencies larger than the reservoir natural frequency. This means that foundation flexibility in general will produce small added damping contribution to the first modal coordinate due to reservoir interaction.

To estimate the loading terms for the first modal equation, the real and imaginary parts of the reservoir-filtered ground motion signal can be computed as a linear combination of the parameters β_1 , β_2 , and β_3 that define the proposed mode shape. **Figure 10** shows the real and imaginary parts of the functions required to compute the frequency-domain hydrodynamic loading coefficients for ground motion in the horizontal and vertical directions,

$$L_{HD1x}(\varpi) = \beta_1 L_{\beta_{1x}}(\varpi) + \beta_2 L_{\beta_{2x}}(\varpi) + \beta_3 L_{\beta_{3x}}(\varpi) \quad (20)$$

$$L_{HD1y}(\varpi) = \beta_1 L_{\beta_{1y}}(\varpi) + \beta_2 L_{\beta_{2y}}(\varpi) + \beta_3 L_{\beta_{3y}}(\varpi) \quad (21)$$

Another alternative approximation for the reservoir-filtered ground motion effects is to assume an incompressible fluid for the loading terms. This leads to frequency-independent terms that allow the assembly of equivalent hydrodynamic masses for horizontal and vertical ground motion components. This assumption simplifies the response computations, in particular in modal spectral analysis. If this approximation is used, the right-hand side term of Eq. (13) is approximated by

$$\begin{aligned} & \left[-\varpi^2 (\mathbf{M}_q - \mathbf{H}_{p,q}(\varpi)) + j\varpi \mathbf{C}_q + \mathbf{K}_q \right] \mathbf{Q}(\varpi) = \\ & -\Phi^T (\mathbf{M} + \mathbf{M}_{HDx}) \mathbf{1}_x \ddot{U}_{gx}(\varpi) - \Phi^T (\mathbf{M} \mathbf{1}_y + \mathbf{M}_{HDy} \mathbf{1}_x) \ddot{U}_{gy}(\varpi) \end{aligned} \quad (22)$$

where the matrices \mathbf{M}_{HDx} and \mathbf{M}_{HDy} represent frequency-independent hydrodynamic mass contributions for horizontal ground motion and vertical ground motion, respectively. Their nonzero entries corresponding to the “wet” lateral-displacement degrees of freedom along the upstream face of the dam, and they can be computed using an incompressible fluid model of the reservoir (Inaudi and Matheu, 2005).

3.5 Higher Mode Correction

Because the second and higher modes of a monolith have natural frequencies significantly higher than the fundamental mode of vibration, their contribution to the response can be estimated by a static mode correction method (Chopra and Fenves, 1986).

In the frequency domain, the higher mode coordinates are assumed uncoupled, therefore

$$\begin{aligned} k_i Q_i(\varpi) = & (-\phi_i^T \mathbf{M} \mathbf{1}_x + H_{p,qi_{gx}}(\varpi)) \ddot{U}_{gx}(\varpi) + \dots \\ & + (-\phi_i^T \mathbf{M} \mathbf{1}_y + H_{p,qi_{gy}}(\varpi)) \ddot{U}_{gy}(\varpi) \quad i = 2, 3, \dots \end{aligned} \quad (23)$$

If the incompressible model is used for the loading terms,

$$\begin{aligned} k_i Q_i(\varpi) = & -\phi_i^T (\mathbf{M} + \mathbf{M}_{HDx}) \mathbf{1}_x \ddot{U}_{gx}(\varpi) + \dots \\ & + -\phi_i^T (\mathbf{M} \mathbf{1}_y + \mathbf{M}_{HDy} \mathbf{1}_x) \ddot{U}_{gy}(\varpi) \quad i = 2, 3, \dots \end{aligned} \quad (24)$$

Several additional criteria can be used to further approximate higher mode components. Details of these procedures are given elsewhere (Inaudi and Matheu, 2005).

3.6 Accuracy of SDOF-Model Estimation

To analyze the prediction capability of the equivalent SDOF model, the FRF from free-field ground acceleration to dam-crest displacement and the FRF from free-field ground acceleration to normalized base shear are computed for the full FE model and for the equivalent SDOF model. The results are shown in **Figure 13** for three values of foundation flexibility. The figures show the exact response of the full model, the estimation using only the contribution of the equivalent first mode, and the estimation using the contribution of the first mode and static correction in higher modes. The input signals are considered without approximations as given by the ground motion acceleration producing inertial forces and the reservoir-filtered ground motion signals. As figures show, dam-crest relative displacement FRF is accurately estimated by the first mode of vibration with or without static correction term. Base shear FRF estimation is significantly improved by including the static correction term in addition to the equivalent single mode response. **Figure 14** compares the simplified method using the full reservoir-filtered ground motion and the simplified method using frequency-independent loading terms. As the figure shows, very similar results are predicted by both methods. Therefore, a simplified method with static correction and incompressible fluid model for the evaluation of loading terms constitutes an efficient alternative for modal spectral analysis of dams on flexible foundation.

4. CONCLUSIONS

Any simplified linear method for dam analysis has its limitations in strong ground motion response estimation: nonlinearities in concrete and rock foundation and fluid cavitation are neglected. Nevertheless, linear models give a good starting point for preliminary dam design. A precise estimation of modes of vibration, with

foundation flexibility effects included, lead to better estimates of inertial forces and hydrodynamic interaction.

The consideration of foundation flexibility in the determination of mode shapes has significant influence on the effective modal mass, hydrodynamic pressure, and base shear in cases of low modulus of elasticity of the foundation rock with respect to dam concrete. The use of the dam-foundation fundamental mode shape instead of the standard fundamental mode (dam on rigid foundation) is recommended for simplified seismic analysis of dams if the foundation modulus of elasticity is of the order or smaller than that of the dam concrete. A simple 3DOF model is proposed for the corresponding implementation of the simplified analysis.

As the examples demonstrated, the approximation of the frequency-domain loading terms by using an incompressible model of the fluid leads to satisfactory results in dams with closed-loop frequencies separated from the reservoir natural frequencies, a typical situation for gravity dams on flexible foundation rock. Research by the authors on these topics is ongoing with the intent of improving valuable simplified linear response spectrum methods available to the engineering community.

5. ACKNOWLEDGEMENTS

This work was sponsored by the U.S. Army Corps of Engineers District, Sacramento, and the Navigation Systems Research Program of the U.S. Army Engineer Research and Development Center. Permission to publish was granted by Director, Geotechnical and Structures Laboratory, U.S. Army Engineer Research and Development Center, Vicksburg, Mississippi, USA.

6. REFERENCES

Department of Defense, "Soil Dynamics and Special Design Aspects," Department of Defense Handbook, MIL-HDBK-1007//3, 1983.

Fenves, G. and Chopra, A.K., "Earthquake Analysis and Response of Concrete Gravity Dams," Report No. UCB/EERC-84/10, University of California, Berkeley, CA, 1984.

Fenves, G. and Chopra, A.K., "Simplified Analysis for Earthquake Resistant Design of Concrete Gravity Dams," Report No. UCB/EERC-85/10, University of California, Berkeley, CA, 1986.

Inaudi J.A. and Matheu, E.E., "Simplified Dynamic Analysis of Concrete Gravity Dams," Technical Report ERDC/GSL TR-##, U.S. Army Engineer Research and Development Center, Geotechnical and Structures Laboratory, Vicksburg, MS, 2005.

Inaudi J.A. and Matusевич, A., "Continuum Models of Unsymmetric Beams," 2005 (in preparation).

Richart, F.E., Woods, R.D., and Hall, J.R., "Vibrations of Soils and Foundations," Prentice-Hall, New Jersey, 1970.

Wolf, J.P. and Meek, J.W., "Foundation Vibration Analysis Using Simple Physical Models", Prentice-Hall, Englewood Cliffs, NJ, 1994.

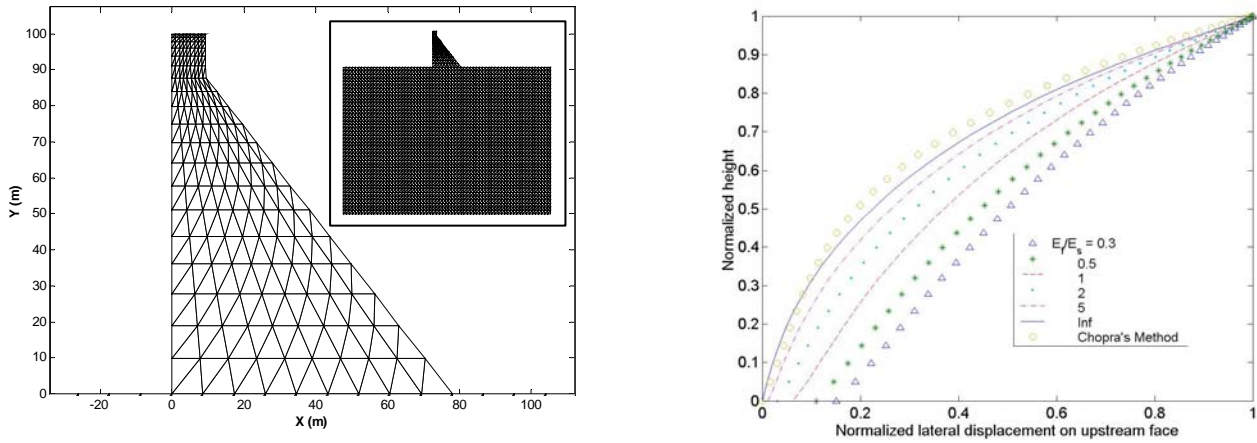


Figure 1. FE-model mesh (left) and fundamental vibration mode shape on upstream face of dam computed with FE model for $E_f / E_s = 0.3, 0.5, 1, 2, 5, \infty$ (right)

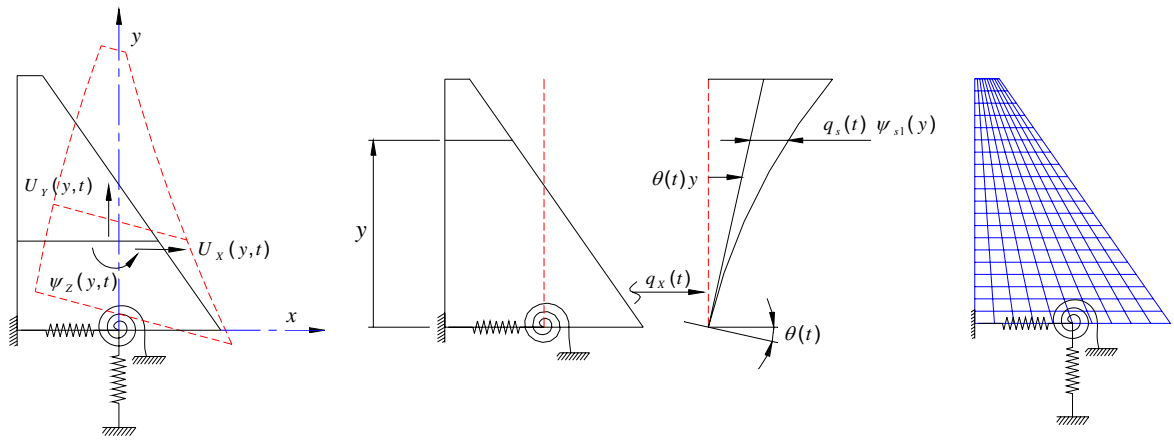


Figure 2. Alternative simplified models of dam-foundation system.

Table 1 Comparison of fundamental period and normalized effective mass for lateral ground motion estimated by 2D FE model, continuum model with lumped foundation model (CP), and 3DOF model with lumped foundation model. Values in parentheses are for foundation stiffness adjusted to 2D FE model.

E_f/E_s	T_1 [s]			m_{e1x}/m_{dam}			m_{e1y}/m_{dam}		
	FE	CP	3DOF	FE	CP	3DOF	FE	CP	3DOF
0.3	0.419	0.340 (0.381)	0.342 (0.385)	0.731	0.665 (0.717)	0.770 (0.832)	0.051	0.064 (0.077)	0 (0)
0.5	0.351	0.291 (0.319)	0.292 (0.322)	0.687	0.621 (0.678)	0.710 (0.779)	0.045	0.056 (0.067)	0 (0)
1	0.291	0.250 (0.266)	0.250 (0.266)	0.604	0.551 (0.604)	0.620 (0.683)	0.038	0.046 (0.054)	0 (0)
2	0.257	0.228 (0.236)	0.228 (0.236)	0.517	0.490 (0.527)	0.547 (0.590)	0.031	0.038 (0.043)	0 (0)
5	0.235	0.215 (0.218)	0.214 (0.218)	0.437	0.440 (0.458)	0.490 (0.511)	0.026	0.032 (0.034)	0 (0)
Inf	0.212	0.206	0.205	0.358	0.400	0.447	0.022	0.028	0

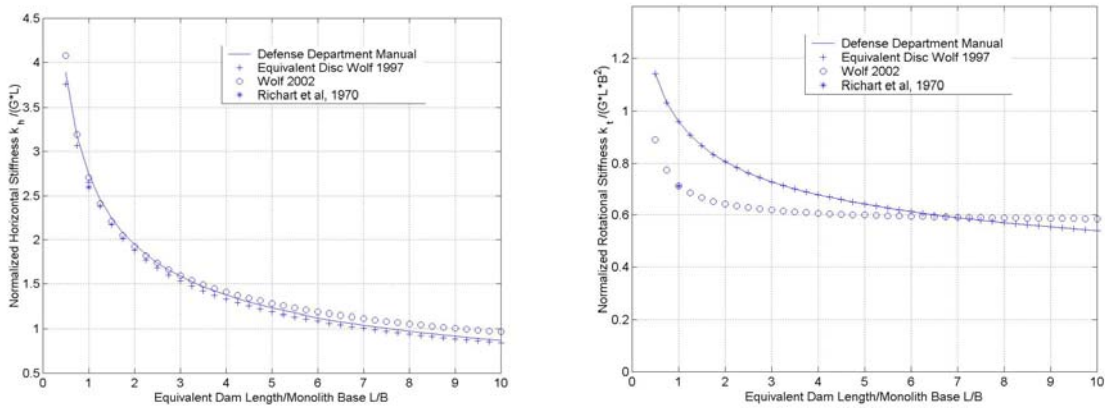


Figure 3. Equivalent foundation stiffness per unit width.

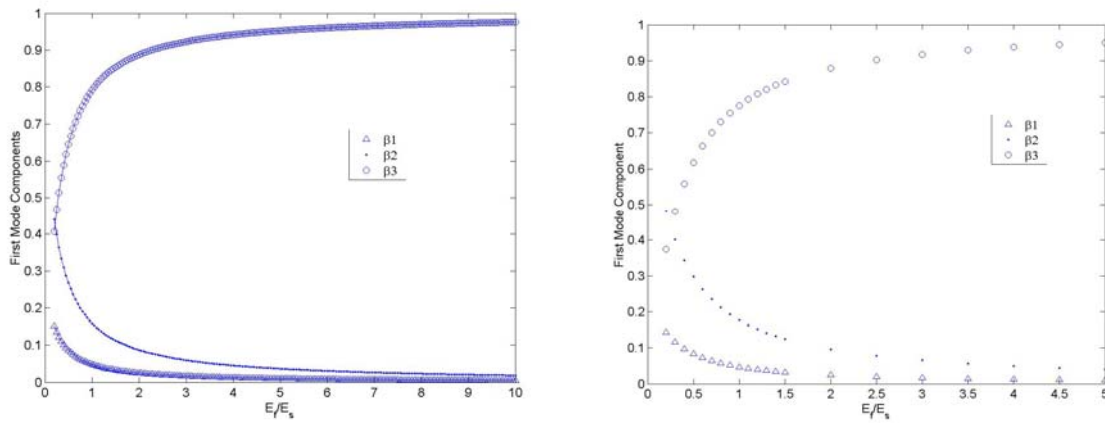


Figure 4. Contributions to lateral displacement of the first mode due to rocking and lateral deformation of the foundation. a) 3DOF model; b) CP model.

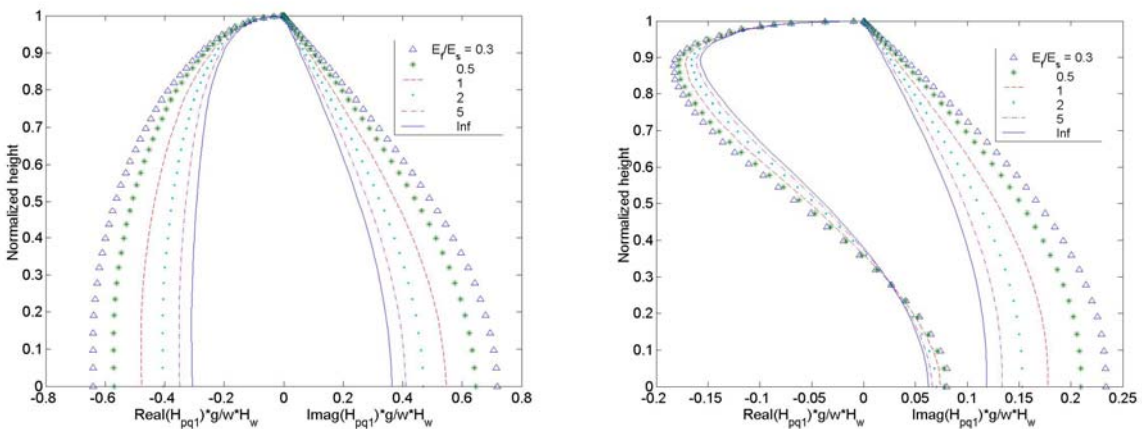


Figure 5. Effect of foundation flexibility on feedback hydrodynamic pressure function for fundamental mode shape: a) $\varpi / \omega_{r1} = 1$, $\alpha = 0.90$; b) $\varpi / \omega_{r1} = 1.5$, $\alpha = 0.90$.

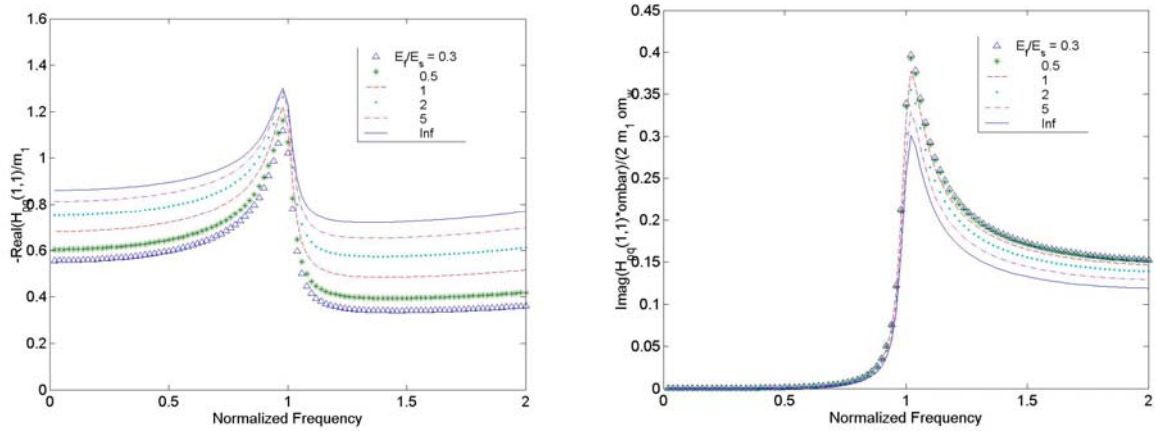


Figure 6. Normalized hydrodynamic mass contribution to first modal coordinate as a function of normalized frequency ϖ / ω_{r1} and damping contribution $\text{Im}(H_{p,q}^{(1,1)})\varpi / (2m_1\omega_{r1})$ ($\alpha = 0.90$).

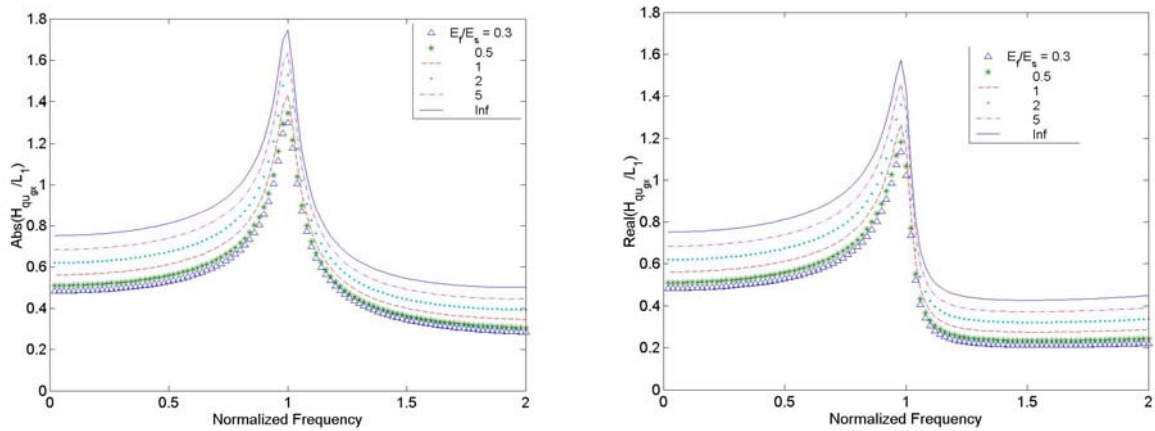


Figure 7. Feed-forward hydrodynamic pressure on the first mode $H_{p,q}^{(1,1)}$ normalized by $L_1 = \phi_1^T \mathbf{M} \mathbf{1}_x$, as a function of normalized frequency ($\alpha = 0.90$): a) absolute value, b) real part.

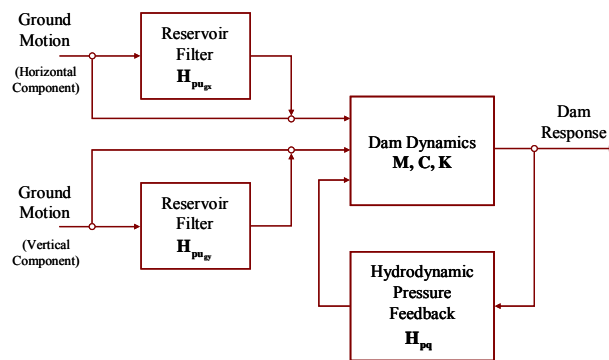


Figure 8. Block diagram representation of dam-reservoir interaction.

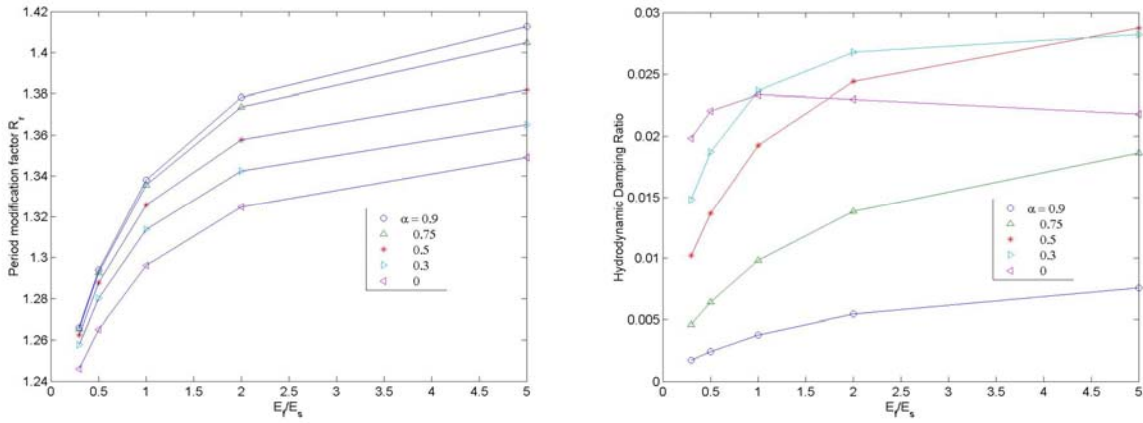


Figure 9. Period modification factor R_r and hydrodynamic damping ratio ξ_r as functions of E_r/E_s for various values of α (First mode of FE model).

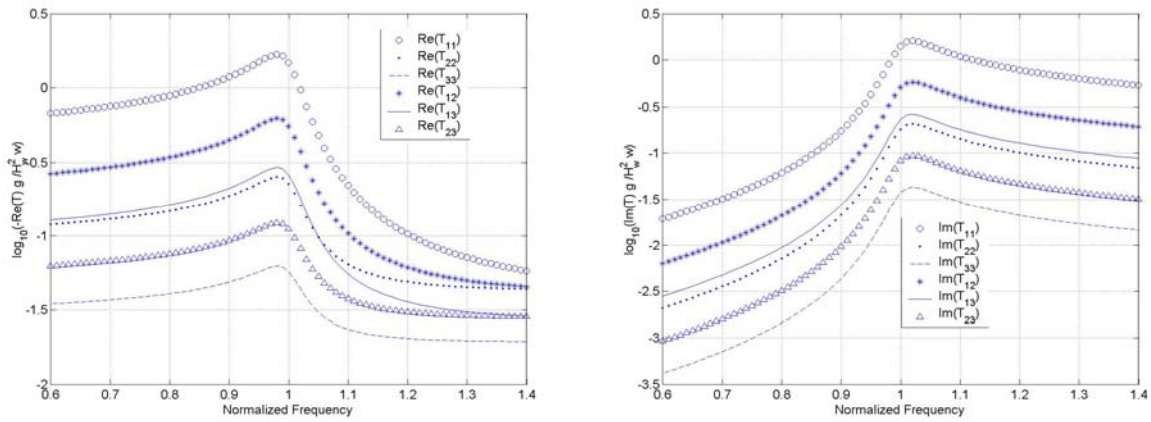


Figure 10. $T_{HD}(\omega)$ for the three generalized mode shapes normalized to unity at dam-crest frequency ($\alpha = 0.90$).

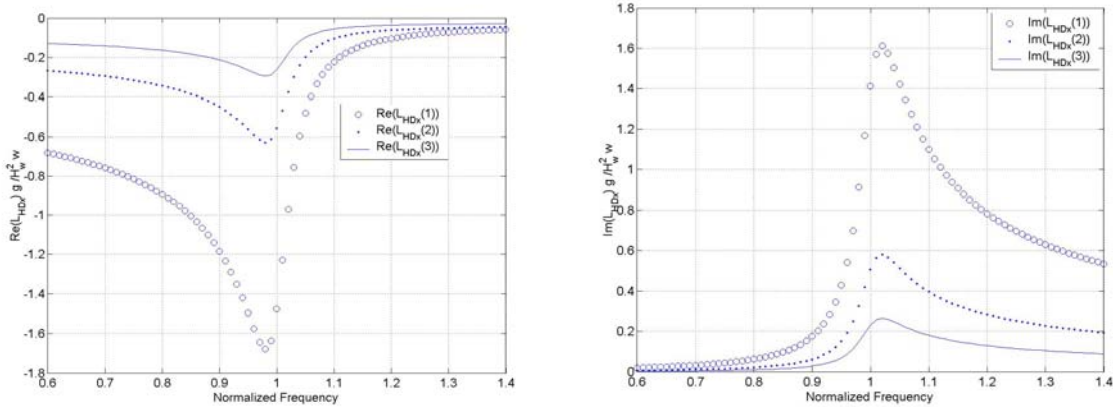


Figure 11. $L_{HDx}(\omega)$ for the three generalized mode shapes normalized to unity at dam-crest frequency ($\alpha = 0.90$).

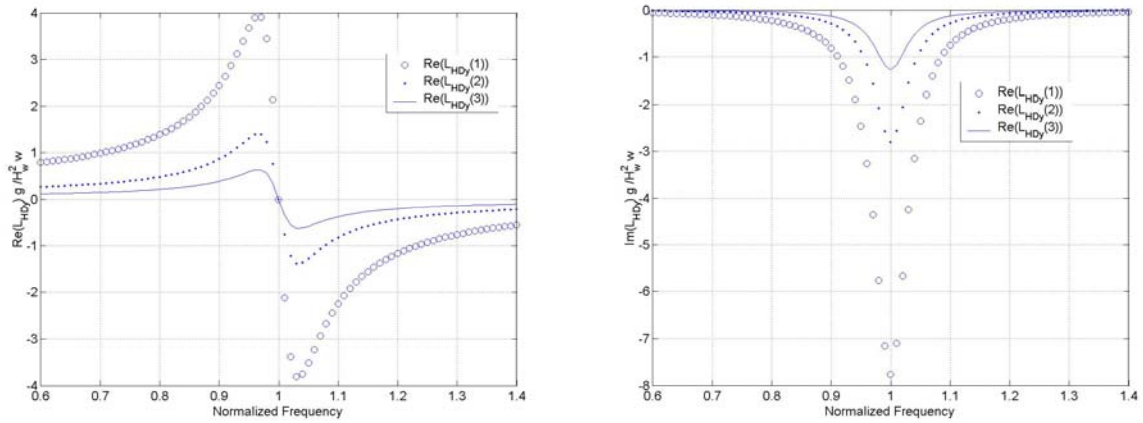


Figure 12. Normalized $L_{HDy}(\omega)$ for the three generalized mode shapes normalized to unity at dam-crest.

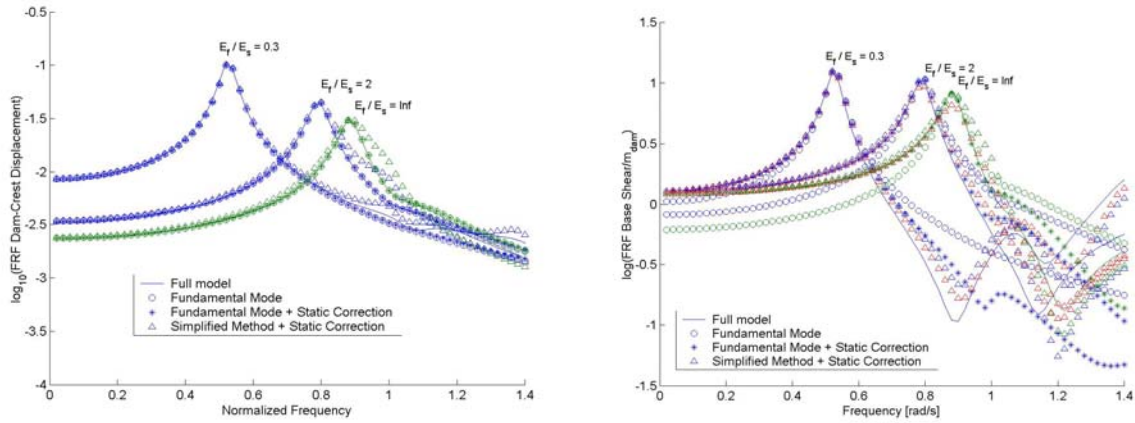


Figure 13. Dam-crest displacement FRF and normalized base-shear FRF for FE model (solid line), single mode ($E_f / E_s = 0.3, 2, \infty$). No foundation radiation damping considered in the analyses; 5% structural damping ratios in all modes.

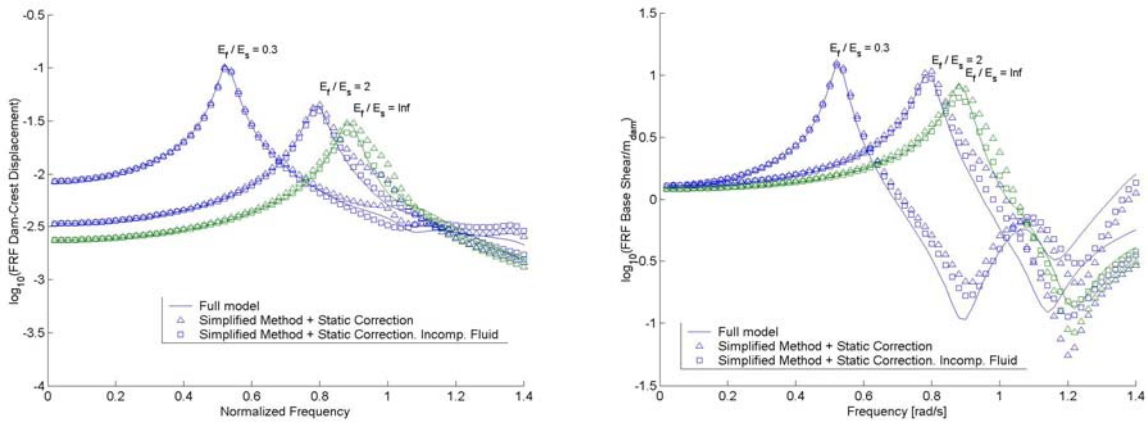


Figure 14. Dam-crest displacement FRF and normalized base-shear FRF for FE model (solid line), simplified method and simplified method with incompressible fluid model for loading terms.